Am J Transl Res 2023;15(4):2703-2715
www.ajtr.org /ISSN:1943-8141/AJTR0147761

Original Article

Celastrol enhances tamoxifen sensitivity in the treatment of triple negative breast cancer via mitochondria mediated apoptosis pathway

Bingjie Qi[1*], Qigao Yan[2*], Pei Zhang[3], Yu Ren[1], Huijuan Liu[4], Tingting Liu[1], Lingli Zhu[1], Yu Chen[1]

[1]College of Pharmacy, Anqing Medical and Pharmaceutical College, Anqing 246000, Anhui, China; [2]Development Planning Division, Anqing Medical and Pharmaceutical College, Anqing 246000, Anhui, China; [3]College of Pharmacy, Bengbu Medical College, Bengbu 233000, Anhui, China; [4]Technology Department, Anqing Medical and Pharmaceutical College, Anqing 246000, Anhui, China. [*]Equal contributors.

Received November 15, 2022; Accepted January 17, 2023; Epub April 15, 2023; Published April 30, 2023

Abstract: Objective: To investigate the enhancement of chemosensitivity of tamoxifen (TAM) in triple negative breast cancer (TNBC) by celastrol (CEL) through mitochondrial mediated pathway. Methods: Human TNBC MDA-MB-231 cells were divided to the control group (medium treatment), TAM-L group (low concentration TAM treatment, 0.5 μM TAM treatment), TAM-H group (1 μM TAM treatment), CEL-L group (low concentration CEL treatment, 1 μM CEL), CEL-H group (high concentration CEL treatment, 3 μM CEL), CEL-L+TAM group (low concentration CEL and TAM co-treatment) and CEL-H+TAM group (high concentration of CEL co-treated with TAM). The proliferation and invasion of cells in each cell group were detected by MTT assay and Transwell assay, respectively. Changes in mitochondrial membrane potential were determined by JC-1 staining. 2'-7'-dichlorofluorescein diacetate (DCFH-DA) fluorescence probe combined with flow cytometry was used to measure the levels of reactive oxygen species (ROS) in cells. The GSH/(GSSG+GSH) level in the cells was detected with glutathione (GSH)/oxidized glutathione (GSSG) enzyme-linked immunosorbent assay (ELISA) kit. The expression levels of the apoptosis-related proteins B lymphocytoma-2 (Bcl-2), Bcl-2-associated X protein (Bax), sheared cysteine-containing aspartate protein hydrolase 3 (Cleaved Caspase-3), and cytochrome C (Cytc) in each group were measured by Western blot. The tumor model of subcutaneous transplantation of TNBC cells in nude mice was established. After administration, the volume and mass of tumors in each group were measured, and the tumor inhibition rate was calculated. Results: Compared with the Control group, cell proliferation inhibition rate (24 h, 48 h), apoptosis rate, ROS level, Bax, cleaved caspase-3 and Cytc protein expression were conspicuously increased in the TAM, CEL-L, CEL-H, CEL-L+TAM and CEL-H+TAM groups (all $P < 0.05$), and cell migration and invasion, mitochondrial membrane potential, GSH level, and Bcl-2 protein expression were conspicuously decreased (all $P < 0.05$). Compared with the TAM group, the cell proliferation inhibition rate (24 h, 48 h), apoptosis rate, ROS level, Bax, cleaved caspase-3 and Cytc protein expression were increased in the CEL-H+TAM group (all $P < 0.05$), and cell migration rate, cell invasion number, mitochondrial membrane potential, GSH level and Bcl-2 protein expression were decreased in the CEL-H+TAM group (all $P < 0.05$). Compared with the CEL-L group, the cell proliferation inhibition rate (24 h, 48 h), apoptosis rate, ROS level, Bax, cleaved caspase-3 and Cytc protein expression were significantly increased in the CEL-H group (all $P < 0.05$), and cell migration rate, cell invasion number, mitochondrial membrane potential, GSH level and Bcl-2 protein expression were decreased in the CEL-H group (all $P < 0.05$). Compared with the model group, the tumor volume of TAM group, CEL-H group, CEL-L+TAM group and CEL-H+TAM group decreased (all $P < 0.05$). Compared with TAM group, the tumor volume in CEL-H+TAM group decreased significantly ($P < 0.05$). Conclusion: CEL can promote apoptosis and enhance the TAM sensitivity in TNBC treatment through a mitochondria-mediated pathway.

Keywords: Celastrol, mitochondrial pathway, triple-negative breast cancer, tamoxifen, drug resistance susceptibility

Introduction

Breast cancer is the most common and fatal malignancy for women worldwide, and its incidence is increasing year by year. As a subtype of breast cancer, triple negative breast cancer (TNBC) refers to estrogen receptor (ER) negative, progesterone receptor (PR) negative and

human epidermal growth factor receptor 2 (HER2) negative as indicated by immunohistochemistry (IHC). TNBC occupies 10-20% of the total breast cancer patients [1-3].

Tamoxifen (TAM) is one of the commonly used drugs for clinical treatment of TNBC. It is an estrogen receptor antagonist that exerts antitumour effects in breast cancer in an estrogen independent manner [4]. Recurrence and metastasis of breast cancer is a great challenge to improve patient survival, and resistance of cancer cells to chemotherapeutic agents is one of the main causes of recurrence and metastasis in TNBC [5]. Therefore, reducing the drug resistance of cancer cells is currently a key clinical issue to improve the effect of cancer treatment. Celastrol (CEL), also known as tripterine, is a quinone methoxy triterpene compound extracted from the rhizomes of Celastrus and Tripterygium. In recent years, researchers have found that CEL has anti-inflammatory, immunosuppressive, and antitumor pharmacological effects [6-8].

Tumorigenesis is usually accompanied by blockage of apoptotic channels, which allows cancer cells to overproduce; therefore, an important way to fight cancer is to promote apoptosis of cancer cells [9]. Mitochondrial apoptosis refers to Bax protein moving to the outer membrane of mitochondria through BH3-only protein and polymerization caused by various apoptotic signals. The formed membrane channel can stimulate mitochondria to release Cyt C and Smac, and Cyt C can form apoptotic bodies with caspase-9, resulting in a series of downstream cascade reactions to regulate cell apoptosis [10]. The mitochondrial apoptotic pathway, as one of the endogenous apoptotic pathways, plays an important role in inhibiting the proliferation of cancer cells and promoting apoptosis [11]. Because there is little research on the anti-tumor mechanism of CEL, this study is intended to investigate whether CEL enhances the chemosensitivity of TNBC cells to TAM through the mitochondrial apoptosis pathway and its specific mechanism of action.

Materials and methods

Cells

Human TNBC cells MDA-MB-231 cells were provided by Shanghai Cell Bank of the Chinese Academy of Sciences.

Animals

Eighty-four 5-week-old SPF female BALB/c-nu nude mice, with a body weight of 18-20 g, were provided by Beijing Weitong Lihua Experimental Animal Technology Co., Ltd. Shanghai Branch, with the license number of SYXK (Shanghai) 2022-0018. All animals were raised in the IVC animal room, provided with free access to food and water. The animals were used for experiments after 7 days of adaptive feeding. This experiment was approved by the Animal Ethics Committee of Anqing Medical College.

Main reagents and instruments

CEL (purity > 98%) was provided by Shanghai Tongtian Biotechnology Co. Trypsin, fetal bovine serum, and high sugar DMEM medium were purchased from Hangzhou Four Seasons Green Bioengineering Materials Co. MTT cell proliferation and cytotoxicity assay kit, crystalline violet staining solution, Annexin V-FITC/PI apoptosis assay kit and JC-1 mitochondrial membrane potential assay kit were purchased from Shanghai Biyuntian Biotechnology Co. Transwell chambers were purchased from Corning Co. Bicinchoninic acid (BCA) protein quantification kit was purchased from Thermo Fisher Scientific, USA. Glutathione (GSH)/oxidized glutathione (GSSG) ELISA kit was provided by Beijing Solabo Technology Co., Ltd; 2'-7'-dichlorofluorescein-diacetate (DCFH-DA) fluorescent probe was purchased from Invitrogen. Tamoxifen, rabbit anti-human B-cell lymphoma 2 (Bcl-2), Bcl-2-associated X protein (Bax), sheared cysteine-containing aspartate protein hydrolase 3 (Cleaved Caspase-3), cytochrome C (Cytc) antibodies and their horseradish peroxidase (HRP)-labeled goat anti-rabbit secondary antibodies were provided by Sigma, USA. M2E multi-functional enzyme labeler was provided by Molecular Device, USA; inverted fluorescence microscope was provided by Leica, Germany; FACS Caliber flow cytometer was provided by Becton Dickinson, USA; Tetra gel electrophoresis instrument was provided by Bio-Rad, USA.

Cell culture

MDA-MB-231 cells were cultured in DMEM medium containing 10% fetal bovine serum in a cell culture incubator at 37°C containing 5% CO_2, and cell growth was closely monitored daily, with fresh medium changed every 2-3

days. Cells in good growth condition and at logarithmic growth stage were used for subsequent experiments.

Cell grouping and treatment

MDA-MB-231 cells at logarithmic growth stage were inoculated in 96-well plates at a density of 1×10^4 cells/well. After being plastered, the cells were divided into control group (blank medium treatment), TAM group (1 μM TAM treatment [12]), CEL-L group (low concentration CEL treatment, 1 μM CEL), CEL-H group (high concentration CEL treatment, 3 μM CEL [13]), CEL-L+TAM group (low concentration of CEL co-treated with TAM), and CEL-H+TAM group (high concentration of CEL co-treated with TAM) for corresponding treatments.

Establishment of TNBC animal model

MDA-MB-231 cells in logarithmic growth phase were collected and digested by adding trypsin, and then resuspended in serum-free medium to prepare cell suspension. The cell concentration was adjusted to 4×10^7 pieces/mL. The single cell suspension was injected under the fourth pair of breast pads on the right side of nude mice, 0.1 mL for each. After inoculation, the mass at the injection site of the nude mice was observed. On the 7th day, the nodule could be touched at the inoculation site, indicating that the modeling was successful.

Animal grouping and administration

A total of 72 nude mice were successfully modeled in this study, and their stacks were integrated into model group, Tam group (50 mg/kg TAM) [14], CEL-L group (5 mg/kg CEL), CEL-H group (10 mg/kg CEL) [15], Tam+CEL-L group, and Tam+CEL-H group. Another 12 mice were used as the normal control. When the tumor volume reached 100 mm^3, each group underwent drug intervention at the corresponding drug dose. CEL was administered by intraperitoneal injection once a day for 14 days. TAMs were administered by intraperitoneal injection once every 2 days for 7 times. Normal group and model group were intraperitoneally injected with the same amount of normal saline.

Determination of cell proliferation by MTT method

MDA-MB-231 cells at logarithmic growth stage were planted in 96-well plates at a density of 1×10^4 cells/well, and after 24 h of incubation, the corresponding concentrations of drugs were added, each group was provided with 6 repeated wells. After 24 h and 48 h of incubation in a cell incubator with 5% CO_2, 10 μL/well of MTT solution was added and the cells were planted in the cell incubator for another 4 h. After that, the supernatant was discarded, 100 μL of DMSO solution was added to each well, placed on a shaker for 10 min, and after waiting for the dissolution of the produced purple crystals, the absorbance value of each well at 490 nm was detected by an enzyme marker to calculate the cell proliferation inhibition rate. Inhibition rate = (1 - OD value of drug-treated group/OD value of control group) × 100%.

Determination of cell migration by scratch assay

Cells at logarithmic growth phase were inoculated in 6-well plates at a density of 5×10^5 cells/well and treated in dofferent groups. After 24 h incubation, the cells were grown to about 80% in confluence, and a scratch was drawn vertically with the tip of a 20 μL pipette, after which the cells were washed with PBS and fresh medium was added to continue the incubation for 48 h. The migration of cells at 0 h and 48 h was observed with an inverted microscope and calculated using Image J software. Migration rate = (width at 0 h - width at 48 h)/width at 0 h × 100%.

Determination of cell invasion by Transwell assay

Cells at logarithmic growth phase were collected and inoculated in the gel-coated upper Transwell chamber with a cell density of 5×10^4 cells/well and the volume of 100 μL. 600 μL of DMEM medium containing 10% fetal bovine serum was added to the lower chamber as chemical elicitor. After incubation for 24 h, the chambers were removed, and 4% paraformaldehyde was added to fix the cells for 20 min, after which the membranes were washed three times with PBS and dyed with crystal violet solution for 30 mins. After the removal of excessive staining solution, the upper layer of cells in the chambers was wiped off with a cotton swab. Cells crossing the membrane were observed using an inverted light microscope, and six fields of view per chamber were randomly selected for photography and cell counting.

Determination of apoptosis by flow cytometry

MDA-MB-231 cells were inoculated in 6-well plates at a density of 5×10^4 cells/well, and the cells were treated accordingly after 24 h of incubation. After continuous culture for 24 h, cells were collected by adding trypsin digestion and washed twice with pre-cooled PBS. According to the instructions of Annexin V-FITC/PI double-staining apoptosis assay kit, 1×10^6 cells were added in a centrifuge tube, 500 μL of binding buffer was added to suspend the cells, and 5 μL of Annexin V-FITC and 5 μL of PI were added for 15 min at room temperature and protected from light. The apoptosis rate was determined by flow cytometry. Under microscope, DAPI staining fluorescence of normal nucleus is blue, and apoptotic cells are brown-yellow.

Determination of cellular mitochondrial membrane potential changes by JC-1 staining method

Cells at logarithmic growth phase were taken and treated accordingly. After 24 h of incubation, cells were digested by adding 0.25% trypsin, washed with PBS, resuspended 2 times by adding 0.5 mL JC-1 buffer, and precipitated by centrifugation. The cells were resuspended by adding appropriate amount of PBS and assayed by flow cytometry. Green fluorescence was detected by FL1 channel and red fluorescence was measured by FL2 channel, and the relative ratio of red to green fluorescence intensity was used to indicate the degree of mitochondrial membrane potential depolarization.

Detection of reactive oxygen species (ROS) and GSH/GSSG levels

The intracellular ROS level was detected by DCFH-DA fluorescence probe and flow cytometry. The intracellular GSH/(GSH+GSSG) level was detected with GSH/GSSG ELISA kit. Cells in logarithmic growth period were treated. After 24 h of treatment, cells were digested, centrifuged and collected, which were then incubated with 5 μMol/L DCFH-DA fluorescence probe at 37°C for 20 min. After being washed three times with serum free DMEM medium, the cells in each group were detected for fluorescence intensity by flow cytometry. Subsequently, the GSH level of cells in each group was detected according to the instructions of GSH/GSSG ELISA kit. First, the total GSH (GSH+GSSG) level was measured, and then an appropriate amount of GSH scavenger was used to remove GSH from the sample, which was the GSSG level. The total GSH (GSH+GSSG) minus the content of oxidized GSSG was the GSH level. High GSH/(GSSG+GSH) level reflected the high level of GSH in cells.

Determination of the expression of proteins related to mitochondrial apoptosis pathway by Western blot

Cells at logarithmic growth phase were taken and treated accordingly. Trypsin was added, cells were collected by digestion and centrifugation, supernatant was collected by adding RIPA lysate, and total cellular protein was extracted. The total protein concentration was measured according to the operating instructions of the BCA protein quantification kit. The quantified protein was subjected to SDS-PAGE gel electrophoresis, after which it was transferred to NC membrane and blocked at 4°C by adding skimmed milk powder. The membranes were washed with TBST, followed by the addition of Bcl-2 (1:1000), Bax (1:1000), cleaved caspase-3 (1:1000) and Cytc (1:500) primary antibodies respectively and incubated at 4°C overnight. On the following day, the membrane was washed with TBST and incubated with horseradish peroxidase-labeled IgG secondary antibody (1:2000) at room temperature for 2 h. Electro-Chemi-Luminescence (ECL) reagent was added for color development, and β-actin protein was used as an internal reference. Exposure was performed under a gel imager, and the grayscale values of the target proteins were calculated and analyzed using Image Lab software.

Determination of tumor volume and mass in tumor bearing mice

All nude mice were sacrificed by cervical dislocation after the end of administration, the tumor tissues were dissected and removed, and the longest diameter (a) and shortest diameter (b) of tumors in tumor bearing mice of each group were determined using vernier calipers, and the tumor volume was calculated. Tumor volume (V) = $ab^2/2$. Tumor inhibition rate was calculated by weighing the tumor mass, and the tumor inhibition rate (%) = (average tumor mass of model group - average tumor mass of dosing group)/average tumor mass of model group × 100%.

Table 1. Comparison of proliferation inhibition rate of MDA-MB-231 cells in each group

Group	Inhibition rate (%)	
	24 h	48 h
Control	0.23±0.01	0.15±0.01
TAM-L	33.42±3.78	52.35±4.87
TAM-H	22.56±3.62$^{*,@}$	38.43±4.25$^{*,@}$
CEL-L	6.21±1.23*	10.30±1.12*
CEL-H	18.25±2.49$^{*,\&}$	30.05±2.94$^{*,\&}$
CEL-L+TAM-H	24.84±2.02*	40.23±3.74*
CEL-H+TAM-H	36.40±3.86$^{*,\#,\wedge}$	57.42±6.10$^{*,\#,\wedge}$

Compared with the Control group, $^{*}P < 0.05$; compared with the TAM-L group, $^{@}P < 0.05$; compared with the TAM-H group, $^{\#}P < 0.05$; compared with the CEL-L group, $^{\&}P < 0.05$; compared with the CEL-H group, $^{\wedge}P < 0.05$. Notes: TAM-L: tamoxifen-L; TAM-H: tamoxifen-H; CEL-L: celastrol-L; CEL-H: celastrol-H; CEL-L+TAM-H: celastrol-L+tamoxifen-H; CEL-H+TAM-H: celastrol-H+tamoxifen-H.

Data statistics and analysis

All experimental data in this study were statistically analyzed using Graph Pad Prism 7.0 software. The experimental data were expressed as mean ± standard deviation (mean ± SD). One-way ANOVA was used for comparison among multiple groups, and LSD-t test was used for further pairwise comparisons. Differences were considered statistically significant at $P < 0.05$.

Results

Comparison of cell proliferation in each group

As shown in **Table 1**, compared with the Control group, the cell proliferation inhibition rate (24 h, 48 h) was significantly higher in the TAM group, CEL-L group, CEL-H group, CEL-L+TAM group, and CEL-H+TAM group (all $P < 0.05$); Compared with TAM-L group, the inhibition rate of cell proliferation (24 h, 48 h) in TAM-H group decreased significantly. Compared with the TAM-H group, the cell proliferation inhibition rate (24 h, 48 h) was significantly higher in the CEL-H+TAM-H group ($P < 0.05$). There was no significant difference in the cell proliferation inhibition rate (24 h, 48 h) between CEL-L+TAM-H group and TAM-H group ($P > 0.05$). Compared with the CEL-L group, the cell proliferation inhibition rate (24 h, 48 h) was significantly higher in the CEL-H group ($P < 0.05$). Compared with the CEL-H group, the cell proliferation inhibition rate (24 h, 48 h) was significantly higher in the CEL-H+TAM-H group ($P < 0.05$). The results showed that the inhibition rate of cell proliferation in TAM group was dose-dependent. With the increase of TAM dosage, the inhibition rate of cell proliferation decreased gradually, indicating that cells developed TAM resistance. In the following experiments, a dose of TAM-H group was selected as the TAM group for research.

Table 2. Comparison of cell migration rate among groups

Group	Cell migration rate (%)
Control	67.89±4.03
TAM	40.30±4.68*
CEL-L	55.68±5.77*
CEL-H	44.94±4.62$^{*,\&}$
CEL-L+TAM	37.92±3.36*
CEL-H+TAM	27.35±2.96$^{*,\#,\wedge}$

Compared with the Control group, $^{*}P < 0.05$; compared with the TAM group, $^{\#}P < 0.05$; compared with the CEL-L group, $^{\&}P < 0.05$; compared with the CEL-H group, $^{\wedge}P < 0.05$. Notes: TAM: tamoxifen; CEL-L: celastrol-L; CEL-H: celastrol-H; CEL-L+TAM: celastrol-L+tamoxifen; CEL-H+TAM: celastrol-H+tamoxifen.

Comparison of cell migration ability among groups

As shown in **Table 2** and **Figure 1**, compared with the Control group, the cell migration rate was significantly lower in the TAM, CEL-L, CEL-H, CEL-L+TAM, and CEL-H+TAM groups (all $P < 0.05$). Compared with the TAM group, the cell migration rate was significantly lower in the CEL-H+TAM group ($P < 0.05$), and there was no significant difference in the cell migration rate between CEL-L+TAM group and TAM group ($P > 0.05$). Compared with the CEL-L group, the cell migration rate was significantly lower in the CEL-H group ($P < 0.05$). Compared with the CEL-H group, the cell migration rate was significantly lower in the CEL-H+TAM group ($P < 0.05$).

Comparison of cell invasion ability among groups

As shown in **Table 3** and **Figure 2**, compared with the Control group, the number of cell invasion was significantly reduced in the TAM, CEL-L, CEL-H, CEL-L+TAM, and CEL-H+TAM groups (all $P < 0.05$). Compared with the TAM group, the number of cell invasion was significantly reduced in the CEL-H+TAM group ($P < 0.05$),

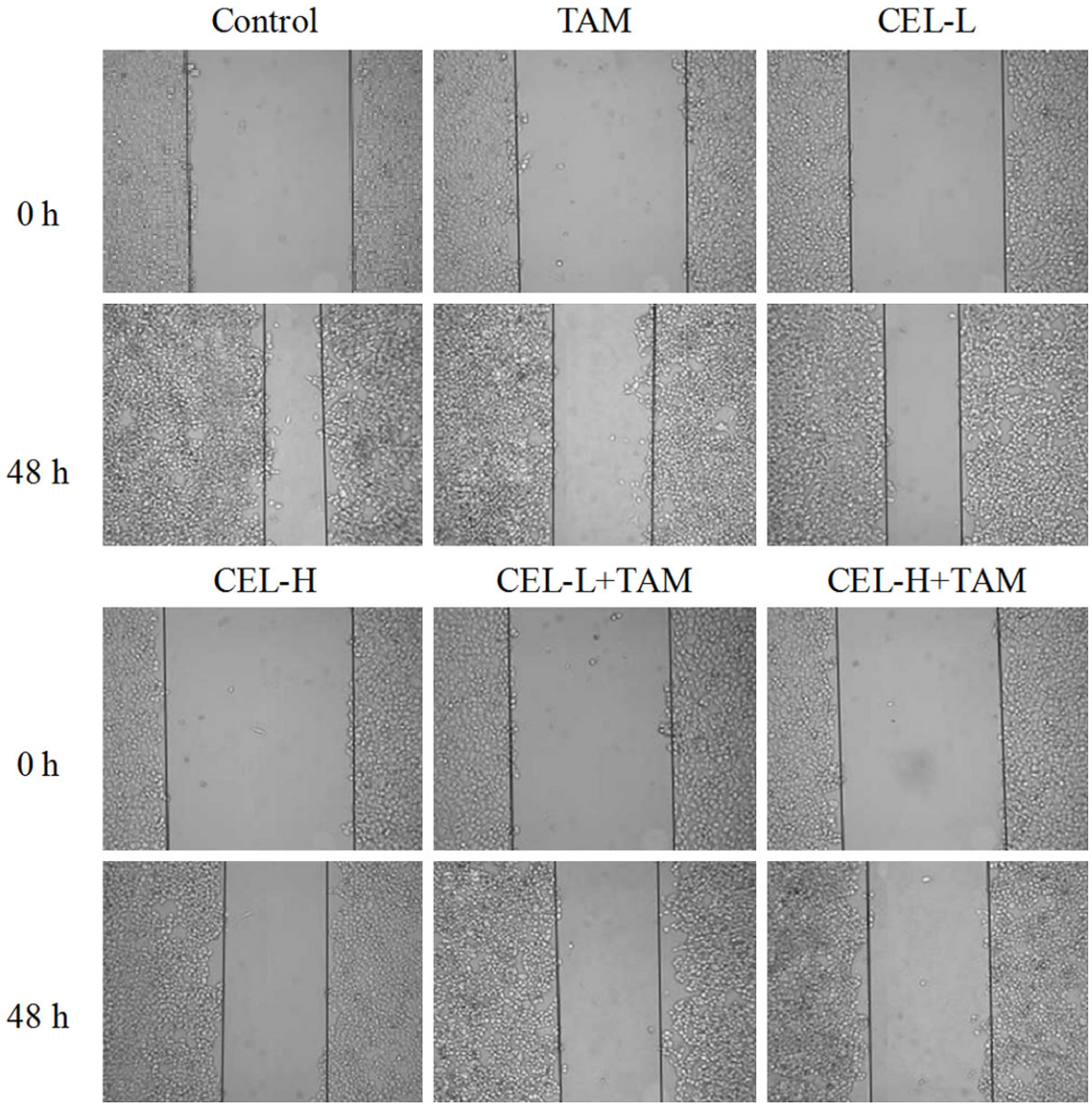

Figure 1. Cell migration detected by cell scratching assay. Notes: TAM: tamoxifen; CEL-L: celastrol-L; CEL-H: celastrol-H; CEL-L+TAM: celastrol-L+tamoxifen; CEL-H+TAM: celastrol-H+tamoxifen.

Table 3. Comparison of cell invasion ability among groups

Group	Number of cell invasion (pcs/field of view)
Control	162.11±14.20
TAM	87.24±9.97*
CEL-L	138.34±14.57*
CEL-H	104.53±12.04*,&
CEL-L+TAM	82.73±9.56*
CEL-H+TAM	52.80±7.84*,#,^

Compared with the Control group, *P < 0.05; compared with the TAM group, #P < 0.05; compared with the CEL-L group, &P < 0.05; compared with the CEL-H group, ^P < 0.05. Notes: TAM: tamoxifen; CEL-L: celastrol-L; CEL-H: celastrol-H; CEL-L+TAM: celastrol-L+tamoxifen; CEL-H+TAM: celastrol-H+tamoxifen.

and there was no significant difference in the number of cell invasion between CEL-L+TAM group and TAM group (P > 0.05). Compared with the CEL-L group, the number of cell invasion was significantly reduced in the CEL-H group (P < 0.05). Compared with the CEL-H group, the number of cell invasion was significantly reduced in the CEL-H+TAM group (P < 0.05).

Comparison of apoptosis rates among groups

As shown in **Table 4** and **Figure 3**, compared with the Control group, the apoptosis rate was significantly higher in the TAM, CEL-L, CEL-H,

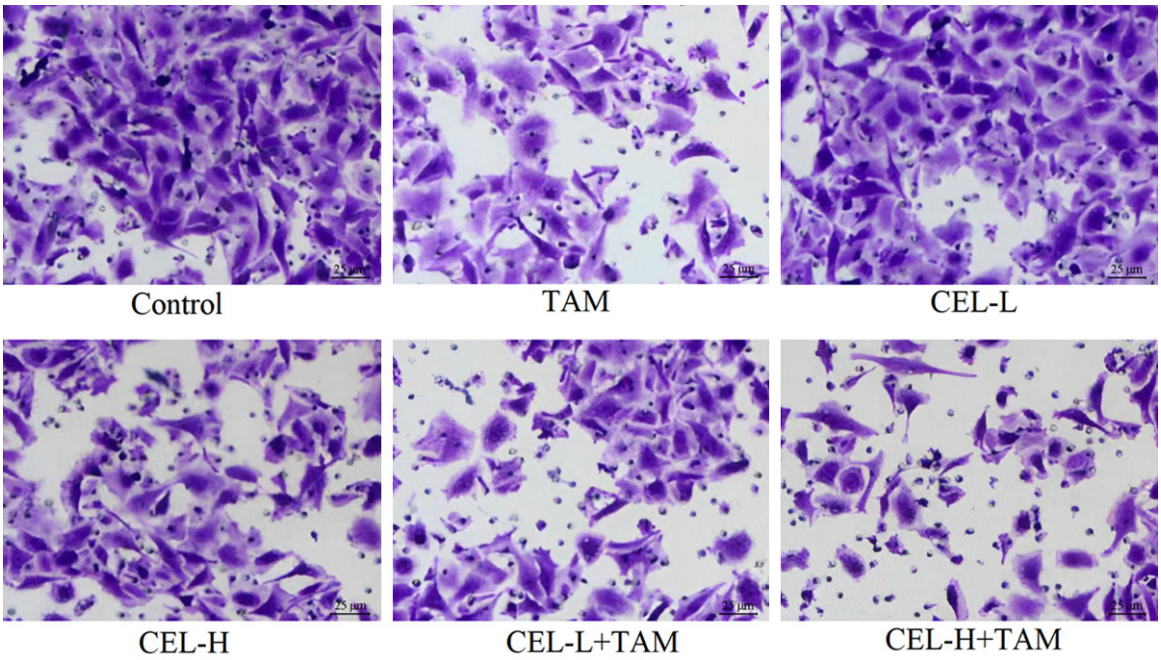

Figure 2. Cell invasion detected by Transwell assay (× 400). Notes: TAM: tamoxifen; CEL-L: celastrol-L; CEL-H: celastrol-H; CEL-L+TAM: celastrol-L+tamoxifen; CEL-H+TAM: celastrol-H+tamoxifen.

Table 4. Comparison of apoptosis rates among groups

Group	Apoptosis rate (%)
Control	3.56±0.39
TAM	28.47±1.77*
CEL-L	11.89±1.14*
CEL-H	22.23±2.01*,&
CEL-L+TAM	30.24±3.89*
CEL-H+TAM	41.92±3.57*,#,^

Compared with the Control group, *P < 0.05; compared with the TAM group, #P < 0.05; compared with the CEL-L group, &P < 0.05; compared with the CEL-H group, ^P < 0.05. Notes: TAM: tamoxifen; CEL-L: celastrol-L; CEL-H: celastrol-H; CEL-L+TAM: celastrol-L+tamoxifen; CEL-H+TAM: celastrol-H+tamoxifen.

CEL-L+TAM, and CEL-H+TAM groups (all P < 0.05). Compared with the TAM group, the apoptosis rate was significantly higher in the CEL-H+TAM group (P < 0.05), and there was no significant difference in the apoptosis rate between CEL-L+TAM group and TAM group (P > 0.05). Compared with the CEL-L group, the apoptosis rate was significantly higher in the CEL-H group (P < 0.05). Compared with the CEL-H group, the apoptosis rate was significantly higher in the CEL-H+TAM group (P < 0.05).

Comparison of mitochondrial membrane potential changes in cells of each group

As shown in **Table 5** and **Figure 4**, compared with the Control group, the mitochondrial membrane potential of cells in the TAM, CEL-L, CEL-H, CEL-L+TAM, and CEL-H+TAM groups decreased significantly (all P < 0.05). Compared with the TAM group, the mitochondrial membrane potential of cells in the CEL-H+TAM group decreased significantly (P < 0.05), and there was no significant difference in the mitochondrial membrane potential of cells between CEL-L+TAM group and TAM group (P > 0.05). Compared with the CEL-L group, the mitochondrial membrane potential of cells in the CEL-H group decreased significantly (P < 0.05). Compared with the CEL-H group, the mitochondrial membrane potential of cells in the CEL-H+TAM group decreased significantly (P < 0.05).

Comparison of ROS and GSH levels in cells of each group

Table 6 shows that compared with the Control group, the cell ROS level in TAM group, CEL-L group, CEL-H group, CEL-L+TAM group and CEL-H+TAM group increased significantly (all P < 0.05), while the GSH level decreased signifi-

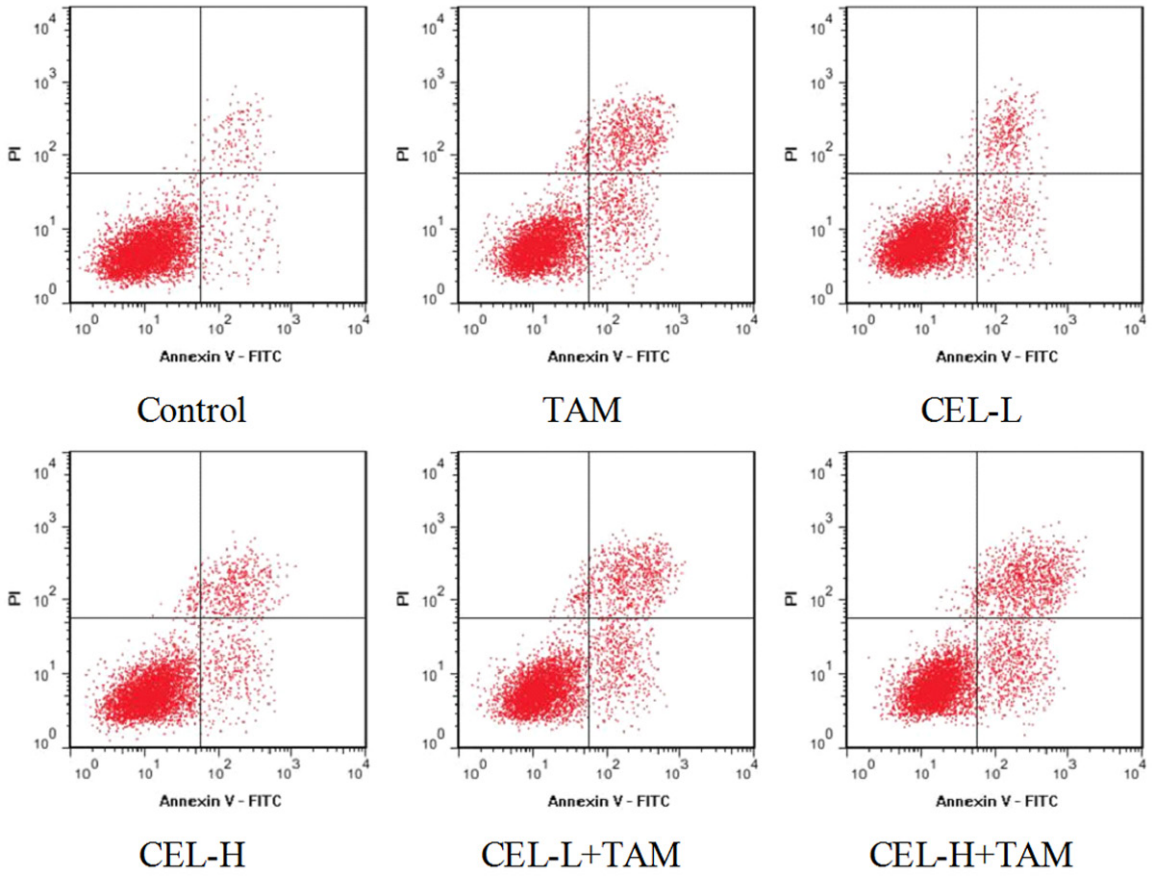

Figure 3. Apoptosis rate detected by flow cytometry. Notes: TAM: tamoxifen; CEL-L: celastrol-L; CEL-H: celastrol-H; CEL-L+TAM: celastrol-L+tamoxifen; CEL-H+TAM: celastrol-H+tamoxifen.

Table 5. Comparison of mitochondrial membrane potential changes among groups

Group	Mitochondrial membrane potential (L2/FL1)
Control	4.38±0.23
TAM	2.07±0.16*
CEL-L	3.41±0.20*
CEL-H	2.36±0.18*,&
CEL-L+TAM	1.98±0.25*
CEL-H+TAM	0.73±0.05*,#,^

Compared with the Control group, *P < 0.05; compared with the TAM group, #P < 0.05; compared with the CEL-L group, &P < 0.05; compared with the CEL-H group, ^P < 0.05. Notes: TAM: tamoxifen; CEL-L: celastrol-L; CEL-H: celastrol-H; CEL-L+TAM: celastrol-L+tamoxifen; CEL-H+TAM: celastrol-H+tamoxifen.

cantly (all P < 0.05). Compared with TAM group, ROS level in CEL-H+TAM group was significantly increased (P < 0.05), while GSH level was significantly decreased (P < 0.05); there was no significant difference in the ROS level and GSH level between CEL-L+TAM group and TAM group (P > 0.05). Compared with CEL-L group, ROS level in CEL-H group increased significantly (P < 0.05), while GSH level decreased significantly (P < 0.05). Compared with CEL-H group, the ROS level of cells in CEL-H+TAM group increased significantly (P < 0.05), while the GSH level decreased significantly (P < 0.05).

Comparison of the expression of mitochondrial apoptosis pathway-related proteins in the cells of each group

As shown in **Table 7** and **Figure 5**, compared with the Control group, Bax, cleaved caspase-3 and Cytc protein expression was significantly higher in cells of the TAM, CEL-L, CEL-H, CEL-L+TAM and CEL-H+TAM groups (all P < 0.05), while Bcl-2 protein expression was significantly lower (all P < 0.05). Compared with the TAM group, Bax, cleaved caspase-3 and Cytc pro-

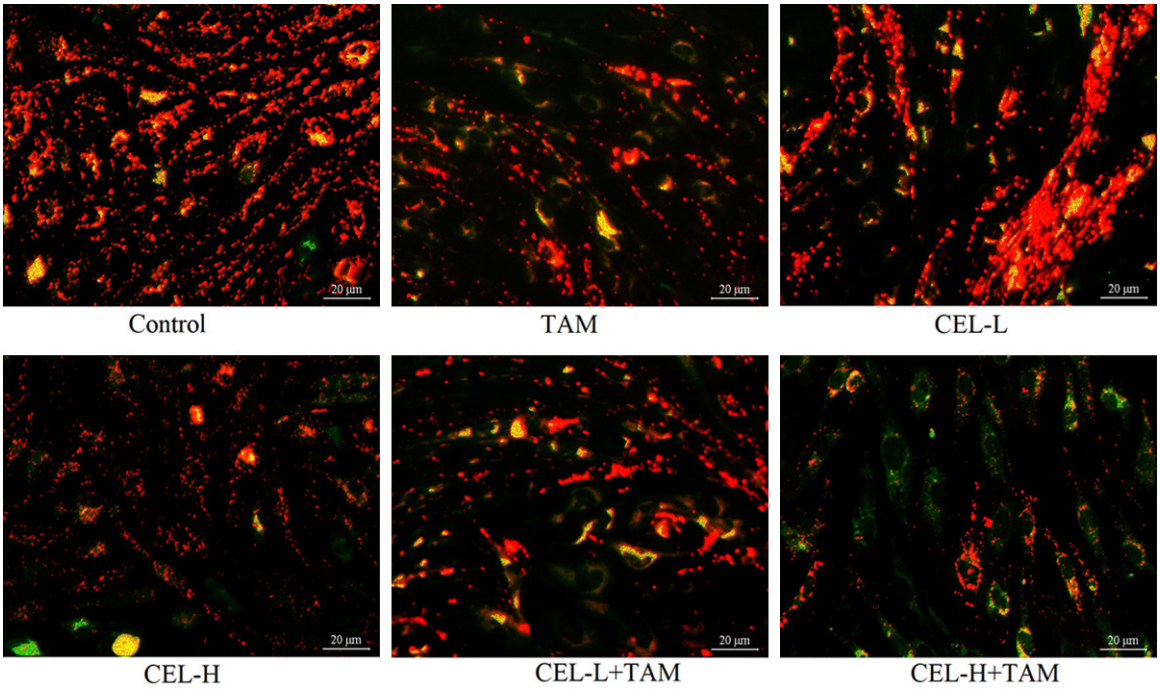

Figure 4. Cellular mitochondrial membrane potential detected by JC-1 staining method (× 400). Notes: TAM: tamoxifen; CEL-L: celastrol-L; CEL-H: celastrol-H; CEL-L+TAM: celastrol-L+tamoxifen; CEL-H+TAM: celastrol-H+tamoxifen.

Table 6. Comparison of ROS and GSH levels in cells among groups

Group	ROS (DCF fluorescence intensity)	GSH (mg GSH/mg total GSH)
Control	15.24±1.20	18.76±1.46
TAM	22.48±1.87*	12.87±0.89*
CEL-L	23.07±2.15*	11.82±1.07*
CEL-H	30.18±2.73$^{*,\&}$	7.08±0.58$^{*,\&}$
CEL-L+TAM	24.24±2.13*	11.38±0.96*
CEL-H+TAM	37.84±3.22$^{*,\#,\wedge}$	3.95±0.27$^{*,\#,\wedge}$

Compared with the Control group, $^{*}P < 0.05$; compared with the TAM group, $^{\#}P < 0.05$; compared with the CEL-L group, $^{\&}P < 0.05$; compared with the CEL-H group, $^{\wedge}P < 0.05$. Notes: TAM: tamoxifen; CEL-L: celastrol-L; CEL-H: celastrol-H; CEL-L+TAM: celastrol-L+tamoxifen; CEL-H+TAM: celastrol-H+tamoxifen.

tein expression was significantly higher (all $P < 0.05$) while Bcl-2 protein expression was significantly lower in the CEL-H+TAM group ($P < 0.05$). There was no significant difference in Bax, cleaved caspase-3 and Cytc protein expression between CEL-L+TAM group and TAM group ($P > 0.05$). Compared with the CEL-L group, Bax, cleaved caspase-3 and Cytc protein expressions were significantly higher (all $P < 0.05$), while Bcl-2 protein expression was significantly lower in the CEL-H group ($P < 0.05$). Compared with the CEL-H group, Bax, cleaved caspase-3 and Cytc protein expression was significantly higher (all $P < 0.05$), and Bcl-2 protein expression was significantly lower in the CEL-H+TAM group ($P < 0.05$).

Comparison of tumor volume and mass of tumor bearing mice in each group

As shown in **Table 8**, compared with the model group, the tumor volume of TAM group, CEL-H group, CEL-L+TAM group and CEL-H+TAM group decreased significantly (all $P < 0.05$). Compared with TAM group, the tumor volume in CEL-H+TAM group decreased significantly ($P < 0.05$), while there was no significant difference in the tumor volume between CEL-L+TAM group and TAM group ($P > 0.05$). Compared with the CEL-L group, the tumor volume in the CEL-H group decreased significantly ($P < 0.05$). Compared with the CEL-H group, the tumor volume in the CEL-H+TAM group decreased significantly ($P < 0.05$).

Discussion

It has been shown that breast cancer has the highest incidence among female cancers, with breast cancer patients accounting for 24.2% of

Table 7. Comparison of expression of mitochondrial apoptosis pathway-related proteins among groups

Group	Bcl-2/β-actin	Bax/β-actin	Cleaved Caspase-3/β-actin	Cytc/β-actin
Control	0.78±0.07	0.34±0.03	0.27±0.03	0.31±0.02
TAM	0.41±0.04*	0.65±0.06*	0.63±0.06*	0.67±0.07*
CEL-L	0.65±0.06*	0.46±0.04*	0.40±0.04*	0.44±0.04*
CEL-H	0.47±0.05*,&	0.60±0.05*,&	0.57±0.05*,&	0.62±0.06*,&
CEL-L+TAM	0.38±0.04*	0.68±0.07*	0.65±0.06*	0.70±0.07*
CEL-H+TAM	0.23±0.02*,#,^	0.84±0.08*,#,^	0.82±0.08*,#,^	0.85±0.07*,#,^

Compared with the Control group, *P < 0.05; compared with the TAM group, #P < 0.05; compared with the CEL group, &P < 0.05; compared with the CEL-H group, ^P < 0.05. Notes: TAM: tamoxifen; CEL-L: celastrol-L; CEL-H: celastrol-H; CEL-L+TAM: celastrol-L+tamoxifen; CEL-H+TAM: celastrol-H+tamoxifen.

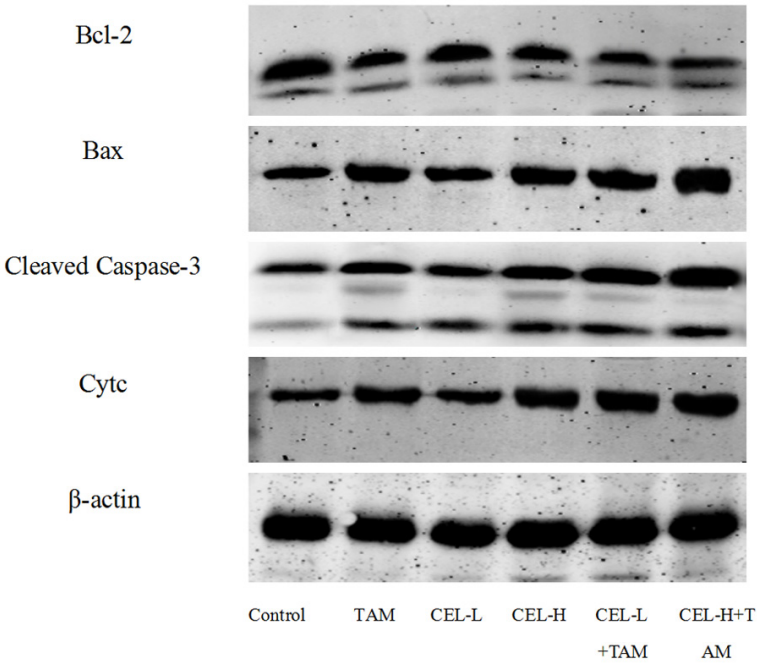

Figure 5. Expression of mitochondrial apoptosis pathway-related proteins detected by Western blot. Notes: TAM: tamoxifen; CEL-L: celastrol-L; CEL-H: celastrol-H; CEL-L+TAM: celastrol-L+tamoxifen; CEL-H+TAM: celastrol-H+tamoxifen.

all cancer patients, including 15.0% of deaths [16]. Breast cancer threatens the life and health of women all over the world. The current clinical reliance on surgical resection, chemotherapy, and radiotherapy of breast cancer has greatly increased the level of diagnosis and treatment of breast cancer and prolonged the survival time of patients. However, the treatment options for TNBC are more limited and have a poor prognosis, and there is significant heterogeneity in the treatment of breast cancer, with different drug resistance [17, 18]. TAM, one of the first-line therapeutic agents for breast cancer, may develop acquired resistance in about 40% of breast cancer patients whose first treatment is effective, which affects the progress and level of breast cancer treatment [19]. Therefore, how to slow down the resistance of chemotherapeutic drugs and increase the sensitivity of tumor cells to chemotherapeutic drugs is of great significance to improve the clinical treatment effect of TNBC.

CEL has been reported to have antitumor effects, inhibit the growth of many types of cancer cells and induce cancer cell death [20]. The antitumor mechanisms of CEL mainly include: inhibition of breast cancer cell growth, metastasis, angiogenesis and promotion of cancer cell apoptosis [21]. It is still therapeutically effective against drug-resistant tumor cell lines and is often used clinically in combination with chemotherapeutic agents such as doxorubicin, paclitaxel, and lapatinib to exert synergistic antitumor effects [22]. Chen et al. [13] found that CEL induces ROS-mediated apoptosis in gastric cancer cells by a mechanism related to direct targeting of peroxiredoxin-2. Ni et al. [23] found that CEL inhibits colon cancer cell growth possibly by negatively regulating miR-21 and PI3K/AKT/GSK-3β pathways. It was shown that compared with the Control group, the proliferation inhibition rate (24 h, 48 h) and apoptosis rate of cells in the CEL-L and CEL-H groups were significantly increased, while the cell migration

Table 8. Comparison of tumor volume and tumor inhibition rate of tumor bearing mice among groups

Group	Tumor volume (mm^3)	Tumor inhibition rate (%)
Normal	0.00±0.00	-
Model	954.26±187.43	-
TAM	528.40±98.57*	43.17
CEL-Low	882.69±158.55	15.63
CEL-High	712.40±116.94*,&	26.85
CEL-Low+TAM	461.52±89.37*	47.20
CEL-High+TAM	276.83±72.60*,#,^	59.38

Compared with the Model group, *P < 0.05; compared with the TAM group, #P < 0.05; compared with the CEL-Low group, &P < 0.05; compared with the CEL-High group, ^P < 0.05. Notes: TAM: tamoxifen; CEL-Low: celastrol-Low; CEL-High: celastrol-High; CEL-Low+TAM: celastrol-Low+tamoxifen; CEL-High+TAM: celastrol-High+tamoxifen.

rate and the number of cell invasion were significantly reduced. The results indicated that CEL had the effect of inhibiting proliferation, migration, invasion and promoting apoptosis in MDA-MB-231 cells, which was consistent with the literature [20]. This study also found that CEL enhanced the chemosensitivity of cells to TAM, and the proliferation inhibition rate (24 h, 48 h) and apoptosis rate of cells in the CEL-H+TAM group were increased, and the cell migration rate and cell invasion number were significantly reduced compared with those in the TAM only group. *In vivo* experiments also showed the same trend.

Apoptosis is influenced and regulated by various signaling pathways, which mainly include the mitochondrial pathway, endoplasmic reticulum stress-mediated apoptosis pathway and death receptor pathway [24-26]. The mitochondrial pathway, as one of the three classical apoptotic pathways, is the central link of apoptosis [27]. When cells undergo apoptosis via the mitochondrial pathway, the morphology of mitochondria undergoes dynamic changes, and the cellular mitochondrial membrane potential is altered [28]. Bcl-2 can inhibit apoptosis and Bax can promote apoptosis. Action of pro-apoptotic factors diminishes the role of Bcl-2 in maintaining the integrity of the mitochondrial membrane, causing Bax to translocate outside the mitochondrial membrane, depolarization of the mitochondrial transmembrane potential and the release of Cytc from the matrix, which activates caspase 3 and other enzymatic systems and allows the cell to initiate apoptosis [29, 30]. In the process of mitochondrial energy production, if the electron transfer of the oxidative respiratory chain is inhibited, the ROS level in the mitochondria will increase, which will activate oxygen free radicals, attack the mitochondrial membrane, cause mitochondrial damage, and increase the mitochondrial membrane permeability [31]. Long term low concentration of ROS can change intracellular signal transduction, which can eventually be adapted by breast cancer cells and make breast cancer cells resistant. This study showed that the mitochondrial membrane potential, cell GSH level and Bcl-2 protein expression in cells of CEL-L and CEL-H groups were decreased, cell ROS level, Bax, cleaved caspase-3 and Cytc protein expression in cells were increased compared with the Control group. Compared with the TAM group, the mitochondrial membrane potential, cell GSH level and Bcl-2 protein expression were decreased in the cells of the CEL-H+TAM group, while cell ROS level, Bax, cleaved caspase-3 and Cytc protein expression were increased. These results suggest that CEL initiates apoptosis via mitochondrial pathway and enhances the chemosensitivity of MDA-MB-231 cells to TAM.

In summary, CEL can enhance the chemosensitivity of TNBC cells to TAM by promoting apoptosis through a mitochondria-mediated pathway. The study provides a new basis and reference for CEL to improve the TAM sensitivity in the treatment of TNBC.

Acknowledgements

Natural Science Foundation Project of Anhui Provincial Department of Education (KJ2021-A1296); Natural Science Foundation Project of Anhui Provincial Department of Education (KJ2021A1292).

Disclosure of conflict of interest

None.

Address correspondence to: Qigao Yan, Development Planning Division, Anqing Medical and Pharmaceutical College, Anqing 246000, Anhui, China. E-mail: bjyqg@163.com

References

[1] Siegel RL, Miller KD and Jemal A. Cancer statistics, 2020. CA Cancer J Clin 2020; 70: 7-30.

[2] Sung H, Ferlay J, Siegel RL, Laversanne M, Soerjomataram I, Jemal A and Bray F. Global cancer statistics 2020: GLOBOCAN estimates of incidence and mortality worldwide for 36 cancers in 185 countries. CA Cancer J Clin 2021; 71: 209-249.

[3] Coughlin SS. Epidemiology of breast cancer in women. Adv Exp Med Biol 2019; 1152: 9-29.

[4] Wang Q, Cheng Y, Wang Y, Fan Y, Li C, Zhang Y, Wang Y, Dong Q, Ma Y, Teng YE, Qu X and Liu Y. Tamoxifen reverses epithelial-mesenchymal transition by demethylating miR-200c in triple-negative breast cancer cells. BMC Cancer 2017; 17: 492.

[5] Fahad Ullah M. Breast cancer: current perspectives on the disease status. Adv Exp Med Biol 2019; 1152: 51-64.

[6] Zhang J, Shan J, Chen X, Li S, Long D and Li Y. Celastrol mediates Th17 and Treg cell generation via metabolic signaling. Biochem Biophys Res Commun 2018; 497: 883-889.

[7] Han XB, Tan Y, Fang YQ and Li F. Protective effects of celastrol against gamma irradiation-induced oxidative stress in human umbilical vein endothelial cells. Exp Ther Med 2018; 16: 685-694.

[8] Ma L, Peng L, Fang S, He B and Liu Z. Celastrol downregulates E2F1 to induce growth inhibitory effects in hepatocellular carcinoma HepG2 cells. Oncol Rep 2017; 38: 2951-2958.

[9] Ma ZJ, Lu L, Yang JJ, Wang XX, Su G, Wang ZL, Chen GH, Sun HM, Wang MY and Yang Y. Lariciresinol induces apoptosis in HepG2 cells via mitochondrial-mediated apoptosis pathway. Eur J Pharmacol 2018; 821: 1-10.

[10] Li H, Xiao Y, Tang L, Zhong F, Huang G, Xu JM, Xu AM, Dai RP and Zhou ZG. Adipocyte fatty acid-binding protein promotes palmitate-induced mitochondrial dysfunction and apoptosis in macrophages. Front Immunol 2018; 9: 81.

[11] Chu Q, Gu X, Zheng Q, Wang J and Zhu H. Mitochondrial mechanisms of apoptosis and necroptosis in liver diseases. Anal Cell Pathol (Amst) 2021; 2021: 8900122.

[12] Wang Y, Yue W, Lang H, Ding X, Chen X and Chen H. Resuming sensitivity of tamoxifen-resistant breast cancer cells to tamoxifen by tetrandrine. Integr Cancer Ther 2021; 20: 1534735421996822.

[13] Chen X, Zhao Y, Luo W, Chen S, Lin F, Zhang X, Fan S, Shen X, Wang Y and Liang G. Celastrol induces ROS-mediated apoptosis via directly targeting peroxiredoxin-2 in gastric cancer cells. Theranostics 2020; 10: 10290-10308.

[14] Wang J, Xie S, Yang J, Xiong H, Jia Y, Zhou Y, Chen Y, Ying X, Chen C, Ye C, Wang L and Zhou J. The long noncoding RNA H19 promotes tamoxifen resistance in breast cancer via autophagy. J Hematol Oncol 2019; 12: 81.

[15] Yang Y, Cheng S, Liang G, Honggang L and Wu H. Celastrol inhibits cancer metastasis by suppressing M2-like polarization of macrophages. Biochem Biophys Res Commun 2018; 503: 414-419.

[16] Bray F, Ferlay J, Soerjomataram I, Siegel RL, Torre LA and Jemal A. Global cancer statistics 2018: GLOBOCAN estimates of incidence and mortality worldwide for 36 cancers in 185 countries. CA Cancer J Clin 2018; 68: 394-424.

[17] Koual M, Tomkiewicz C, Cano-Sancho G, Antignac JP, Bats AS and Coumoul X. Environmental chemicals, breast cancer progression and drug resistance. Environ Health 2020; 19: 117.

[18] Xu X, Zhang L, He X, Zhang P, Sun C, Xu X, Lu Y and Li F. TGF-beta plays a vital role in triple-negative breast cancer (TNBC) drug-resistance through regulating stemness, EMT and apoptosis. Biochem Biophys Res Commun 2018; 502: 160-165.

[19] Prashanth Kumar BN, Rajput S, Bharti R, Parida S and Mandal M. BI2536-A PLK inhibitor augments paclitaxel efficacy in suppressing tamoxifen induced senescence and resistance in breast cancer cells. Biomed Pharmacother 2015; 74: 124-132.

[20] Chen SR, Dai Y, Zhao J, Lin L, Wang Y and Wang Y. A mechanistic overview of triptolide and celastrol, natural products from tripterygium wilfordii hook F. Front Pharmacol 2018; 9: 104.

[21] Kashyap D, Sharma A, Tuli HS, Sak K, Mukherjee T and Bishayee A. Molecular targets of celastrol in cancer: recent trends and advancements. Crit Rev Oncol Hematol 2018; 128: 70-81.

[22] Kim SH, Kang JG, Kim CS, Ihm SH, Choi MG, Yoo HJ and Lee SJ. Cytotoxic effect of celastrol alone or in combination with paclitaxel on anaplastic thyroid carcinoma cells. Tumour Biol 2017; 39: 1010428317698369.

[23] Ni H, Han Y and Jin X. Celastrol inhibits colon cancer cell proliferation by downregulating miR-21 and PI3K/AKT/GSK-3β pathway. Int J Clin Exp Pathol 2019; 12: 808-816.

[24] Gu J, Rauniyar S, Wang Y, Zhan W, Ye C, Ji S and Liu G. Chrysophanol induced glioma cells apoptosis via activation of mitochondrial apoptosis pathway. Bioengineered 2021; 12: 6855-6868.

[25] Green DR. The death receptor pathway of apoptosis. Cold Spring Harb Perspect Biol 2022; 14: a041053.

[26] Hu H, Tian M, Ding C and Yu S. The C/EBP Homologous Protein (CHOP) transcription factor functions in endoplasmic reticulum stress-induced apoptosis and microbial infection. Front Immunol 2018; 9: 3083.
[27] Guan Y, Zhao X, Song N, Cui Y and Chang Y. Albicanol antagonizes CD-induced apoptosis through a NO/iNOS-regulated mitochondrial pathway in chicken liver cells. Food Funct 2021; 12: 1757-1768.
[28] Rizwan H, Pal S, Sabnam S and Pal A. High glucose augments ROS generation regulates mitochondrial dysfunction and apoptosis via stress signalling cascades in keratinocytes. Life Sci 2020; 241: 117148.
[29] Zhang Y, Yang X, Ge X and Zhang F. Puerarin attenuates neurological deficits via Bcl-2/Bax/cleaved caspase-3 and Sirt3/SOD2 apoptotic pathways in subarachnoid hemorrhage mice. Biomed Pharmacother 2019; 109: 726-733.
[30] Luo Y, Fu X, Ru R, Han B, Zhang F, Yuan L, Men H, Zhang S, Tian S, Dong B and Meng M. CpG oligodeoxynucleotides induces apoptosis of human bladder cancer cells via Caspase-3-Bax/Bcl-2-p53 axis. Arch Med Res 2020; 51: 233-244.
[31] Ismail T, Kim Y, Lee H, Lee DS and Lee HS. Interplay between mitochondrial peroxiredoxins and ROS in cancer development and progression. Int J Mol Sci 2019; 20: 4407.